Available online at www.sciencedirect.com
SCIENCE DIRECT®
PERGAMON
International Journal of Impact Engineering 28 (2003) 557–574
INTERNATIONAL JOURNAL OF IMPACT ENGINEERING
www.elsevier.com/locate/ijimpeng

Penetration resistance of laminated ceramic/polymer structures

S. Yadav*, G. Ravichandran

Graduate Aeronautical Laboratories, California Institute of Technology, Pasadena, CA 91125, USA

Received 23 January 2001; received in revised form 29 November 2001; accepted 20 August 2002

Abstract

Ballistic penetration experiments have been performed on ceramic tiles laminated with thin layers of polymer in between. The experiment involves shooting a cylindrical rod made of a tungsten heavy alloy (WHA) against an unconfined ceramic/polymer laminated structure that is backed by a 6061-T6 aluminum alloy cylindrical-block, at a velocity ranging between 1000 to 1200 m/s. The residual depth of penetration in the aluminum block is used as a measure of the resistance offered by the laminated ceramic/polymer structure to ballistic penetration. Penetration resistance of the laminated ceramic/polymer structures is compared to that of monolithic ceramic structures of the same total thickness. Experimental results demonstrate that penetration resistance of an unconfined ceramic structure can be improved significantly by laminating ceramic tiles with thin polymer layers in between. This enhanced performance of the laminated structure is attributed to a reduced wave propagation (and damage) velocity in the laminated ceramic/polymer structure and also to the crack arresting feature of the polymer layer.

1. Introduction

Due to their low density but high compressive strength and hardness, ceramic materials have been considered for lightweight armor applications for the past three decades or so. In fact, the first major reported use of ceramic for armor applications dates back to the early 1960s when it was used for helicopter armor and personnel armor. The developed armor consisted of a composite system of boron carbide (B_4C) ceramic bonded to a fiberglass or Kevlar backing and covered with a fabric spall shield. This ceramic composite armor system was significantly lighter than a metallic armor that would be required to provide similar protection against small arms

*Corresponding author. Present address. Fermi National Accelerator Laboratory, MS 316, P.O. Box 500, Wilson & Kirk Roads, Batavia, IL 60510, USA. Tel.: +1-630-840-6490; fax: +1-630-840-8036.
E-mail address: syadav@fnal.gov (S. Yadav).

0734-743X/02/$ - see front matter
PII: S0734-743X(02)00122-7

armor-piercing projectiles. A brief review of the progress made in the use of ceramics for armor applications can be found in [1].

The advances in the processing techniques over the past few decades have further lead to the availability of lower cost ceramic materials. This has lead to a wide utilization of ceramic composite armors in both military and non-military applications. Numerous advances have been made in reducing the areal density of the ceramic composite armor systems. The majority of these efforts have been directed in two distinct directions: (a) synthesizing new ceramic materials with improved mechanical properties, and (b) synthesizing stiffer backing materials to better support the ceramic. However, an alternative approach of reducing the areal density of a ceramic composite armor system is to use a laminated ceramic/polymer structure where the ceramic tiles are laminated with very thin layers (<1 mm) of polymer in between. Although laminated glass/polymer structures have been extensively used as transparent bullet-proof armor against lower caliber threats, there has been no prior work in the open literature on the penetration resistance of ceramic structures laminated with thin polymer layers. The main advantage of a ceramic armor over the transparent glass armor is its protection capability against greater threats such as depleted uranium and tungsten heavy alloy penetrators.

This paper presents the results of penetration experiments performed on unconfined ceramic structures laminated with very thin (0.254 mm) layers of polymer in between. The ballistic performance of the laminated ceramic/polymer structures is compared to that of monolithic ceramic targets of the same thickness. Experimental results show that penetration resistance of the unconfined ceramic targets can be improved significantly by lamination. The basic mechanisms responsible for the enhanced performance of the laminated structures are discussed in this paper. The rest of the paper is divided as follows. Section 2 provides a summary of the prior research work performed on monolithic ceramic materials which is relevant to our understanding of the ballistic behavior of laminated ceramic/polymer structures. A brief discussion on laminated media is also presented in this Section. The experimental methodology adopted in this study, along with a description of the materials used is presented in Section 3. Section 4 presents the experimental results on the monolithic and laminated structures and discusses the mechanisms responsible for the enhanced penetration resistance of the laminated ceramic/polymer structures. Finally, the conclusions derived from this study are summarized in Section 5.

2. Background

This section presents a synopsis of the relevant literature on mechanical behavior of monolithic and laminated ceramic structures. Several studies have been performed to understand the influence of material properties and test conditions on the penetration resistance of monolithic ceramic materials and are discussed in Section 2.1. In contrast, to the best knowledge of the authors, there has been no previous work in the open literature on the penetration behavior of laminated ceramic/polymer structures. Other relevant work on laminated media is presented in Section 2.2. It should be noted that ballistic penetration of ceramics is a complex field of endeavor and sometimes various researchers have proposed alternative explanations for nominally the same phenomenon. This should be kept in mind while going through this section.

2.1. Monolithic ceramic

Several studies have been performed to determine the material parameters that influence the penetration resistance of monolithic ceramic targets. For example, Rosenberg and Yeshurun [2] indicated that the ballistic resistance of a ceramic material could be related to an effective strength parameter defined as an average of the static and dynamic compressive strength of the ceramic. On the other hand, Woodward [3] proposed that the Vickers diamond-pyramid hardness data of a ceramic divided by some factor between 1.0 and 2.9 is an appropriate strength parameter for the ceramic. Sternberg [4] has also examined the material properties that determine the resistance of a ceramic to high-velocity penetration and indicates that the initial resistance to penetration might be governed by the indentation hardness, but the penetration resistance drops to some lower value as cracking in the ceramic precedes penetration. It should be noted that the nucleation and growth of cracks in stress fields ahead of the damage front (penetrator/target interface) has been observed experimentally by Hornemann et al. [5] using high-speed photography during ballistic impact of glass plates. They indicated that the appropriate strength value should be a function of the initial impact velocity, being low at low velocities where cracking can precede penetration, but higher as velocity increases closer to the rate of propagation of the damage front.

Sternberg [4] has proposed that the ballistic performance of a given ceramic material may increase with an increase in the ceramic toughness. However, computational modeling of impact damage in brittle materials indicate that the fracture energy amounts to an exceedingly small fraction ($<1.5\%$) of the initial kinetic energy [6]. The major energy dissipating mechanisms are the kinetic energy picked up by the ceramic fragments and the plastic deformation of the penetrator. Curran et al. [7] have proposed a theoretical micromechanics based model for the comminution and granular flow of brittle material that occurs during ballistic impact on confined ceramic targets. They inferred that the most important ceramic properties determining its penetration resistance are the friction between the comminuted granules, the unconfined compressive strength of the intact material, and the compressive strength of the comminuted material. In contrast, Cortes et al. [8] numerically investigated penetration by cylindrical projectiles of thin, unconfined ceramic tiles backed by thin metallic plates and concluded that the fracture kinetics of ceramic under tension controls its ballistic performance. It was observed that the frictional effects in the comminuted ceramic did not play as significant of a role as the fracture kinetics of the ceramic due to the fairly unconfined state of the comminuted ceramic.

It should be noted that when a ceramic target is impacted by a long-rod penetrator, a divergent spherical wave propagates within the ceramic which is followed by the slower mechanical penetration of the penetrator. It has been observed (e.g. [6]) that the principal stresses near the shock wave front are predominantly compressive in nature. Past investigations have shown that damage in the form of microcracking and/or microplasticity plays an important role in the deformation and failure of ceramics and ceramic composites under dynamic compressive loading conditions [9–12]. The damage evolution under the applied loading is intimately related to microcracking at defects such as pores, inclusions, second phase particles, twin/grain boundary intersections and triple-point grain boundary junctions. The brittle compressive failure process of ceramics has been supported experimentally by observations of loss of the spall strength in numerous ceramics when shock compressed above the Hugoniot elastic limit. Thus, damage can occur in a ceramic target when impacted by a long-rod penetrator, much ahead of the penetrator/

target interface. This could influence the resistance offered by a ceramic armor to long-rod penetration. For example, Hauver [13] observed a decrease in the target resistance (R_t) during long-rod penetration into thick ceramic tiles.

For brittle materials, the target resistance (R_t) may depend on the initial impact velocity and the velocity at which damage propagates within the material. Relatively little is known about velocity at which damage can propagate within a brittle material. For linearly elastic solids, the Rayleigh wave speed, c_R is the theoretical limit of crack propagation speed, and in most materials the maximum speed for crack propagation has been observed to be only a fraction (0.3–0.5) of the Rayleigh wave speed, c_R. For stress levels below the Hugoniot elastic limit, certain researchers (e.g. [14]) have observed propagation of a delayed front of fracture (called as failure wave) following the initial elastic compression wave. Raiser and Clifton [15] have proposed that the failure waves travel at a velocity closer to the Rayleigh wave speed. However, the evidence for this result in not yet convincing and it has been suggested by Grady [16] that the failure waves can propagate at any velocity up to the longitudinal wave velocity in the material. Grady also suggested that damage could initiate in ceramics immediately after the passage of the elastic shock front and that the observed delay time between the shock wave and the failure wave is governed by the kinetics of crack nucleation and growth. Strassburger et al. [17] conducted an experimental study of damage propagation in three different ceramics when impacted by steel projectiles. They observed that the damage velocity, defined as the velocity of the fastest fracture experimentally observed, increased with increasing impact velocity. This would imply that the resistance of ceramics to penetration should decrease with increasing impact velocity. Such a behavior has been observed experimentally by Subramanian and Bless [18] where they observed a decrease in the effective target resistance (R_t) values with increasing impact velocity for alumina targets. At very high impact velocities, Strassburger et al. [17] report damage velocities approaching the longitudinal wave velocity in the ceramic.

2.2. Laminated media

The transmission of mechanical waves through a laminated structure has been studied quite extensively during the last 40 years (e.g., [19–22]). It has been observed that weakly coupled periodic structures are dispersive in nature and a sharp distinction is observed between frequency bands exhibiting wave propagation without attenuation (passing bands) and those showing attenuation and no propagation (stopping bands). Robinson and Leppelmeier [23] provided experimental evidence for the existence of stopping bands and passing bands in layered composites. The quality of the interlamina bond has a significant influence on the dispersive characteristics of wave propagation, as demonstrated by Sotiropoulos [21].

A one-dimensional and a two-dimensional axisymmetric analysis of propagation of transient linear elastic waves in a periodic structure has been performed by El-Raheb [24–26]. In one dimension, El-Raheb considered transient wave propagation in a weakly coupled periodic stack of n hard ceramic layers bonded by $(n-1)$ weak polymer layers and showed that such structures exhibit dispersion due to the periodicity of the structure. The peak normal (compressive) stresses along the stack were observed to attenuate along the stack due to the spreading of the pulse because of the different phase and group velocity of the pulse. A two-dimensional analysis of the same problem demonstrated increased attenuation of the peak normal stresses along the stack

because of radial spreading from the flexural waves. El-Raheb and Tham [27] performed non-destructive experiments on periodic stacks of aluminum nitride (AlN) tiles bonded by thin weak silicone glue. The pressure at the interface of the ceramic and bond layers was measured by carbon gauges along the centerline of the stack. An attenuation of the interface pressure along the stack was observed and the measured experimental histories showed a close match to the two-dimensional analysis by El-Raheb [25].

Cook and Gordon [28] have proposed that large increases in the strength and toughness of brittle solids could be achieved by introducing a "plane of weakness" in the path of a propagating crack to deflect the crack along the interface. Kendall [29] conducted a theoretical analysis to derive a crack deflection criterion for diversion of a Griffith crack along weak, perpendicular interfaces. It was shown that the crack deflection phenomenon depends mainly on the ratio of interface and cohesive fracture energies for the material and the speed of crack propagation. It has been indicated that the failure modes in a laminated material are governed by the interfacial toughness and defects and the thickness and failure strengths of the individual layers [30–32]. A review article on the various laminar design approaches for achieving improvements in the strength and toughness of ceramics, including the incorporation of weak interlayers to induce crack deflection can be found in [33].

Flocker and Dharni [34,35] have investigated the propagation of stress waves in a laminated glass subjected to low-velocity impact for architectural glazing applications. They investigated the influence of the thickness of the glass and polymer layers and the viscoelastic properties of the polymer on stress wave propagation through a three-layer system. It should be noted that the damage tolerance of a laminated glass can be significantly improved by an astute choice of the material and geometrical properties of the laminated system.

3. Experimental methods

This section presents a brief discussion of the experimental methodology adopted in this study along with a description of the penetrator and target materials and the target design.

3.1. Test methodology

Fig. 1 shows a schematic of the test methodology used in this investigation. The experiment involves shooting a tungsten heavy alloy (WHA) rod through an unconfined monolithic or laminated aluminum nitride (AlN) ceramic structure bonded to a 6061-T6 aluminum alloy cylindrical block. The aluminum block is sectioned after the test to measure the residual depth of penetration (DOP) of the penetrator. Penetration resistance of the different laminated structures could then be assessed from the DOP measurements. It should be noted that no lateral (radial) confinement or confinement from cover plate was used for the ceramic laminates. In a recent study by Franzen et al. [36], the ballistic performance of ceramic materials was observed to increase with increasing degree of lateral confinement. The ballistic performance was also observed to be a function of the hardness and thickness of the cover plate. Since it is very difficult to quantify the effects of confinement due to lateral support or due to a front cover plate, we propose to conduct DOP tests on ceramic materials without any confinement. Such a test methodology would be

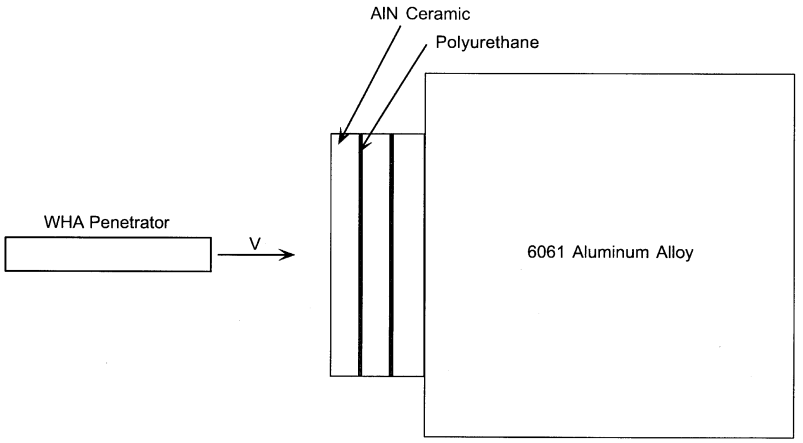

Fig. 1. Schematic representation of the DOP experiments. The experiment involves shooting a WHA penetrator against an unconfined laminated ceramic/polymer structure that is backed by a 6061-T6 aluminum alloy cylindrical block.

useful in comparing experimental results from different laboratories and would remove variability in the observed experimental results, obtained by different researchers, due to the differences in the confinement techniques.

3.2. Material description

3.2.1. Penetrator material

The experiments were performed using a cylindrical WHA penetrator with a flat nose, a length to diameter (L/D) ratio of 6, and a diameter of 8.43 mm. The total mass of the penetrator was 50 gm. It should be noted that for impact on ceramics with sufficiently high strength compared to the penetrator strength, Woodward et al. [37] observed no differences in the ballistic behavior of pointed and blunt penetrators. For such a case it is believed that the ceramic strength is sufficient to fracture the nose of the pointed penetrator and hence a pointed penetrator would have behavior similar to that of a blunt penetrator. The WHA used for the tests, WN308F, was obtained in an as-swaged condition from Osram Sylvania. The material received as a round bar of diameter 11.43 mm was center-less ground to the final diameter of 8.43 mm. The alloy had a density of 17.69 g/cm^3 and a chemical composition of 93 wt% tungsten, 5.6 wt % nickel and 1.4 wt% iron. The hardness measured using the Rockwell C scale was R_c 42. Table 1 lists some of the other relevant mechanical properties for this alloy.

3.2.2. Target material

The experiments were performed on 101.6 mm × 101.6 mm (4″ × 4″) AlN ceramic tiles of different thicknesses. The monolithic ceramic tiles used had a thickness of 38.1 mm (1.5″). Laminated ceramic/polymer structures of total thickness same as that of the monolithic ceramic were fabricated from ceramic tiles of 12.7 mm (0.5″) and 6.35 mm (0.25″) thicknesses. The ceramic tiles, as supplied by the Dow Chemical Company, had an average density of 3.3 g/cm^3 and were manufactured by sintering. A 0.254 mm (0.010″) thick polyurethane film obtained from Deerfield

Urethane, Inc. was used for laminating the ceramic tiles. The polymer film had a density of 1.21 g/cm^3, with a shore hardness of 95 Shore A and an ultimate tensile strength of 69 MPa. Table 1 provides a summary of the mechanical properties of the penetrator and target materials used in this study. Laminated ceramic/polymer structures were obtained by heating the assembly in a furnace under constant applied pressure followed by air cooling. No other adhesive was used in making the laminates.

3.3. Impact facility and target design

The tungsten alloy penetrator was launched down a 3-m long smooth bore barrel (of inside diameter 35 mm) of a powder gun using a sabot assembly shown in Fig. 2. The total mass of the launch package was about 115 g. The distance between the gun muzzle and the target was less than 0.5 m. Therefore, mechanical separation of the penetrator from sabot was obtained rather than aerodynamic separation. This was achieved by using a metal plate with a hole large enough to allow the penetrator to pass through but not large enough for the pusher plate and the sabot. The sabot thus separated did not impact the ceramic target. Fig. 3 shows a schematic representation of such a target design. The stability of the penetrator after separation was tested

Table 1
Mechanical properties

Material	Young's modulus E (GPa)	Density ρ (g/cm^3)	Yield strength (MPa)	Ultimate tensile strength (MPa)	Strain to failure
WHA	345	17.69	1300	1400	0.08
AlN	310	3.3	–	350–400	0.001–0.002
Polyurethane	2.3	1.21	–	69	6.5
6061-T6 Al	69	2.7	276	311	0.2

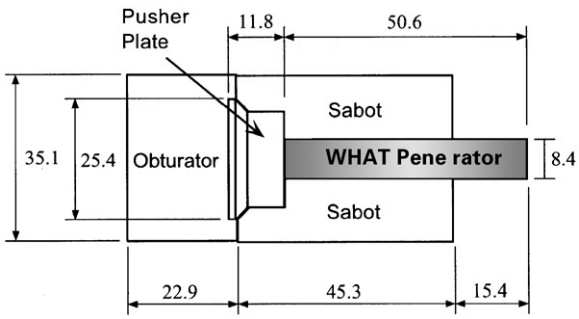

Fig. 2. Schematic representation of the launch package. The WHA penetrator is backed by a titanium alloy pusher plate. The sabot and the obturator are made of plastics. All dimensions are in mm.

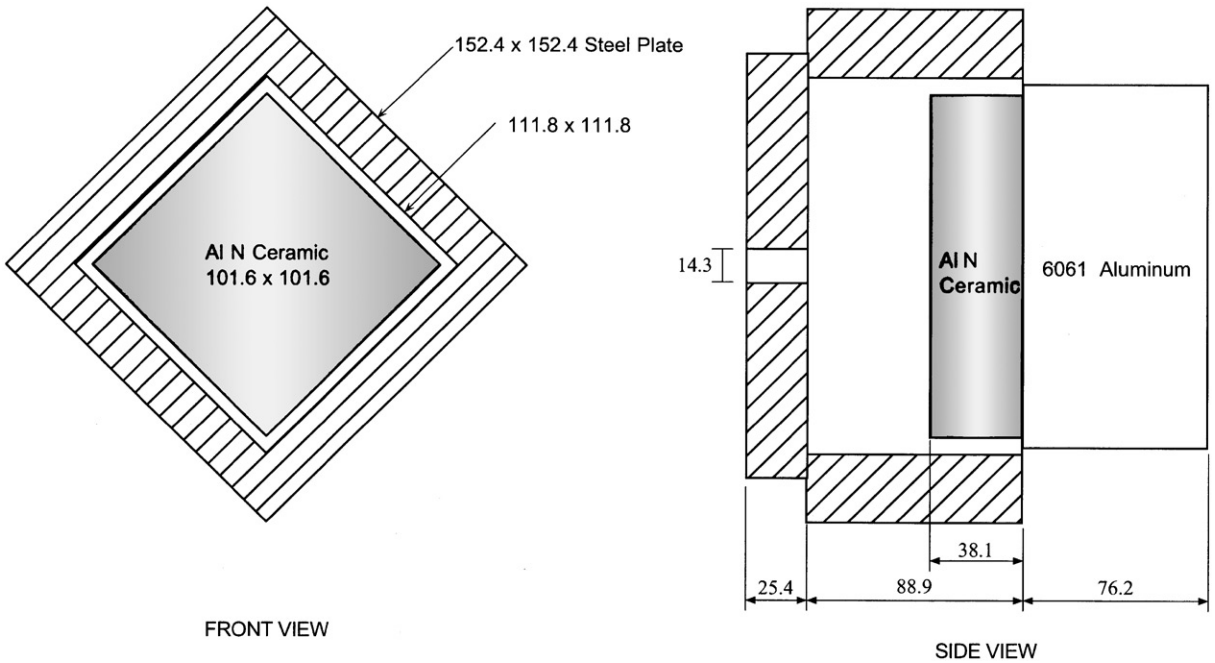

Fig. 3. Schematic representation of the target design. Mechanical separation of the penetrator from sabot is obtained using a mild steel frame with a cover plate. All dimensions are in mm.

by performing several shots on aluminum target blocks (with no ceramic) and sectioning them after the tests to examine the penetration cavity. The sectioned aluminum blocks showed that the penetrator essentially followed a straight path for all the shots. Thus, no destabilization of the penetrator was observed due to the forceful mechanical stripping procedure. Hence, no attempt was made to measure the pitch and yaw of the projectile. Also note that no appreciable pitch and yaw in the projectile is expected to occur within such short flight distances (less than 0.5 m).

The monolithic or the laminated ceramic structure (101.6 mm × 101.6 mm × 38.1 mm thick) was glued to a 152.4 mm (6.0″) diameter and 76.2 mm (3.0″) long 6061-T6 aluminum alloy block using a very thin layer of a two-component epoxy. To absorb the impact energy, the back of the aluminum block was attached to an industrial grade shock absorber. The ceramic–aluminum block assembly was chained down to a V-block that was firmly attached to the target chamber using a fixture. A 127 mm × 127 mm (5.0″ × 5.0″) × 25.4 mm (1.0″) thick mild steel plate with a central hole of diameter 14.3 mm was welded to a mild steel frame of dimensions as shown in Fig. 3. This whole frame rested on the V-block with the back surface of the frame glued to the front face of the aluminum block using a two-component epoxy. Note that there is a clearance between the confining frame and the ceramic target such that the frame provides no radial or front confinement to the ceramic target. The reasons for using the frame were twofold: (a) for mechanical stripping of the sabot, and (b) for containing the post-test ceramic rubble to prevent damage to the target chamber and the fiber-optic cables used for measuring the penetrator velocity. Before impact, the center of the hole on the front plate was aligned mechanically to the

center of the gun barrel. The residual DOP measurements were made by sectioning the backup aluminum block using a band-saw. It should be noted that no bulging of the rear surface of the aluminum block was observed and hence, the assumption of semi-infinite backup plate holds true. In the absence of any confinement, the tested ceramic was totally fragmented and no post-mortem examination of the penetration cavity in the ceramic could be made.

4. Experimental results and discussion

We first present the results of DOP experiments performed on the 6061-T6 aluminum alloy backup block, followed by the shots performed on the monolithic and the laminated ceramic/polymer structures. Experimental results indicate that the penetration resistance of ceramics could be increased significantly by lamination, and possible mechanics-based explanations for this phenomenon are presented. Finally, the effect of the ceramic tile thickness and polymer bond properties on depth of penetration is discussed.

4.1. Baseline tests

In order to obtain a quantitative measure of performance of the monolithic and laminated ceramic structures, some baseline shots were performed to measure the depth of penetration of tungsten alloy penetrators into 6061-T6 aluminum backup blocks, at different impact velocities. Fig. 4 plots the normalized penetration length (penetration depth, P normalized by the initial length, L of the penetrator) versus the initial impact velocity of the tungsten penetrator. A linear

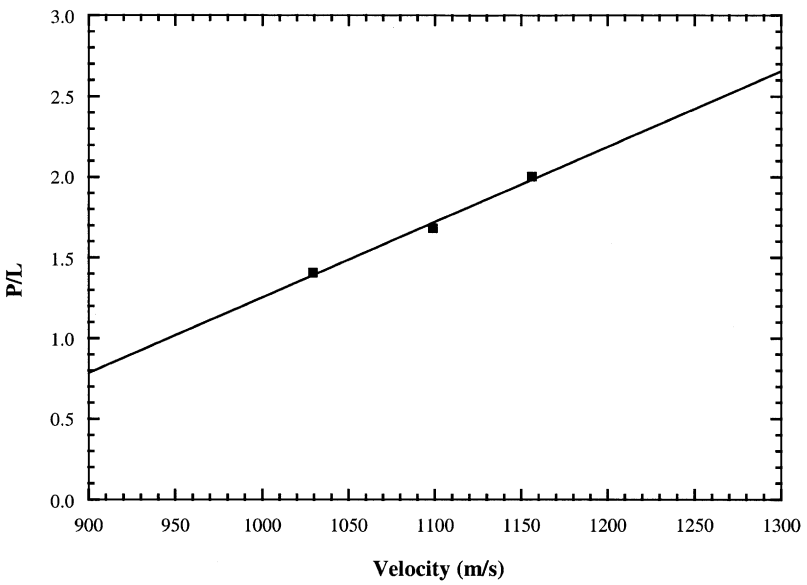

Fig. 4. Plot of the normalized penetration length (P/L) in a 6061-T6 aluminum alloy versus the impact velocity (V).

least-square curve was fitted through the experimental data and is represented by the solid line in Fig. 4. From results of the curve fit, the normalized DOP in 6061-T6 aluminum could be represented by the following expression:

$$\frac{P}{L} = 0.0043 \times V(\mathrm{m/s}) - 3.024. \tag{1}$$

Note that a linear fit to the experimental data is a good approximation to the actual behavior only for the range of velocities considered here. The fit should not be extrapolated to very high velocities where saturation in the depth of penetration values has been observed experimentally. Also note that the fit is only valid for tungsten alloy penetrators with a length-to-diameter (L/D) ratio of 6. It has been observed experimentally by other researchers that shorter L/D penetrators yield a larger value of the normalized penetration length, P/L when compared to large L/D penetrators [38].

4.2. Ceramic tests

Table 2 provides a summary of the DOP shots performed on the monolithic and laminated ceramic/polymer structures, for a fixed ceramic thickness of 38.1 mm. In the table, P_r represents the residual DOP of the penetrator in the 6061-T6 aluminum alloy backup block after having penetrated through the ceramic target. For each impact velocity V, the depth of penetration, P_∞ in a 6061-T6 aluminum block without any ceramic in front is also computed from Eq. (1) and listed in the table. An efficiency factor, η can then be defined as follows:

$$\eta = 1 - \frac{P_r}{P_\infty} \tag{2}$$

Table 2
Summary of the depth of penetration experiments

Shot No.	AlN laminated structure–No. of tiles × tile thickness (mm)	Velocity, V (m/s)	Residual penetration, P_r (mm)	P_∞ (mm)	$\eta = 1 - \frac{P_r}{P_\infty}$
S32	1 × 38.1	1070	12.2	79.7	0.85
S40	1 × 38.1	1121	34.0	90.8	0.63
S38	1 × 38.1	1140	34.5	94.9	0.64
S41	1 × 38.1	1163	30.0	99.9	0.70
S31	3 × 12.7	1045	0	74.3	1.00
S37	3 × 12.7	1102	18.3	86.7	0.79
S43	3 × 12.7	1133	19.8	93.4	0.79
S45	3 × 12.7	1170	26.2	101.5	0.74
S44	3 × 12.7	1176	26.2	102.8	0.75
S49	6 × 6.35	1160	33.5	99.3	0.66
S42	6 × 6.35	1170	39.1	101.5	0.62

and is useful for comparing the effectiveness of ceramic armors of a fixed thickness for different impact velocities. η could also be used to compare the relative performance of monolithic and laminated ceramic targets of the same material and thickness, for different impact velocities. A value of efficiency factor, η equal to one signifies complete protection by the ceramic armor for the given impact velocity with no residual penetration in the backup aluminum block. Thus, higher values of η indicate higher penetration resistance provided by the ceramic armor and vice versa. The efficiency factor, η has been computed for all the shots and is listed in Table 2. The experimental results show that the penetration resistance decreases with an increase in the impact velocity for both the monolithic and laminated ceramic structures. This is consistent with the hypothesis that the effective target resistance decreases as the impact velocity increases (for example, see, [18]) because the damage velocity also increases with impact velocity, as observed by Strassburger et al. [17].

The experimental results from Table 2 are shown graphically in Fig. 5, which shows a plot of the residual penetration P_r versus the impact velocity V for the three different thicknesses of ceramic tiles. An interesting observation from Table 2 and Fig. 5 is that the penetration resistance of the laminated ceramic/polymer structures comprised of three 12.7 mm (0.5″) thick AlN tiles is more than the penetration resistance of the monolithic, 38.1 mm (1.5″) thick AlN ceramic. A limited number of experiments performed on laminated structures comprised of six 6.35 mm (0.25″) thick AlN tiles indicate that the resistance to penetration decreases with any further increase in layering, and approaches values similar to that of the monolithic ceramic at comparable impact velocities. Fig. 6 shows photographs of the sectioned aluminum backup block for the monolithic, 38.1 mm thick AlN tile and for the laminated ceramic/polymer structures comprised of three 12.7 mm thick AlN tiles and six 6.35 mm thick AlN tiles, at a comparable impact velocity. It is again observed that the depth of penetration in the ceramic/polymer structure comprised of three 12.7 mm thick AlN tiles is smaller than the penetration depth in the

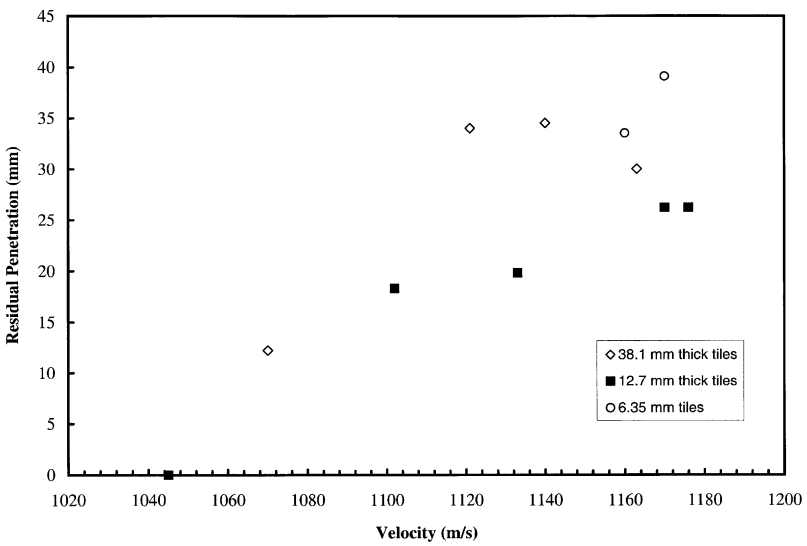

Fig. 5. Plot of residual penetration versus the impact velocity for the three different thicknesses of ceramic tiles.

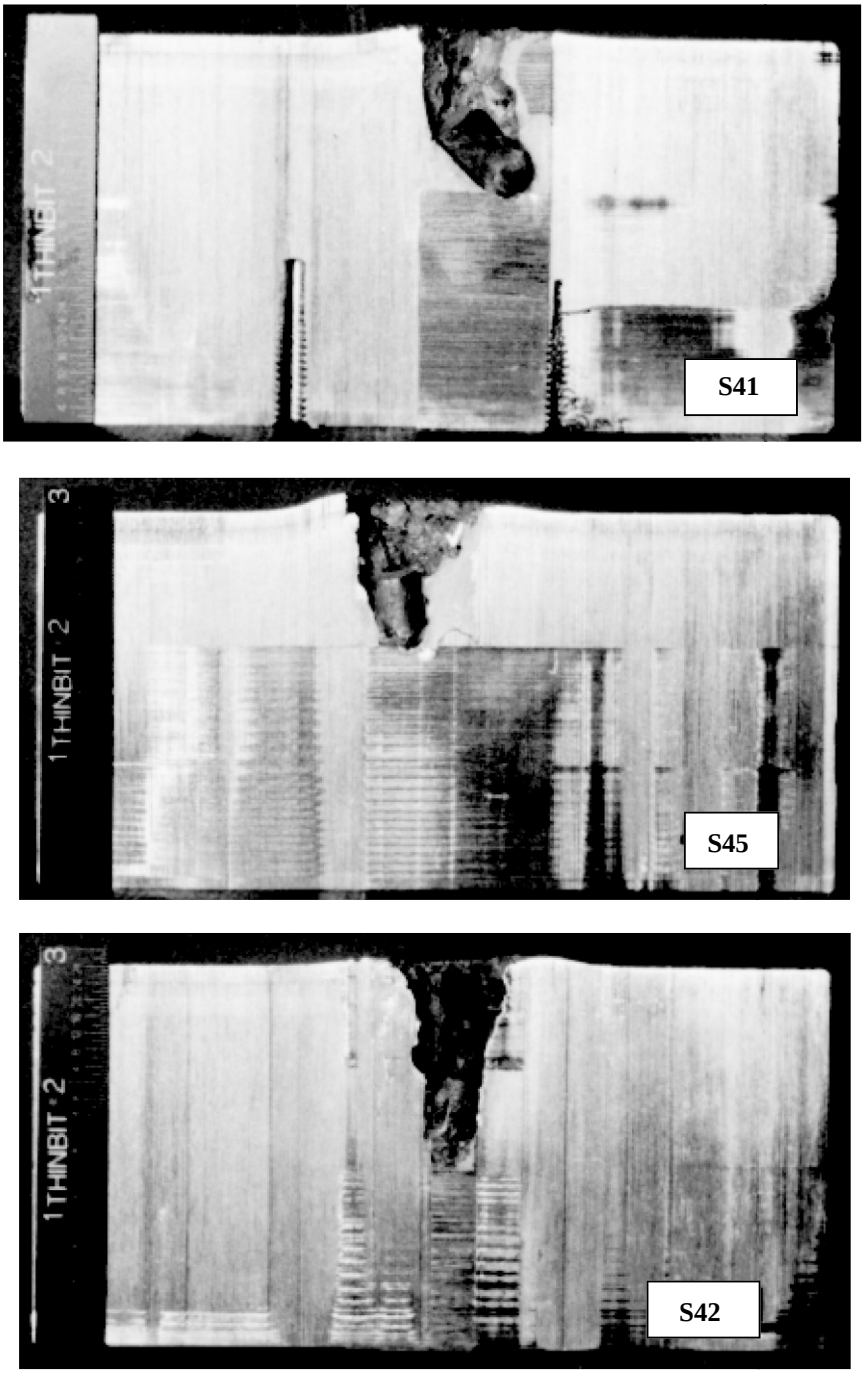

Fig. 6. Comparative performance of the monolithic and laminated ceramic/polymer structures at comparable impact velocity: (a) $V = 1163$ m/s, DOP = 30.0 mm for a 38.1 mm thick monolithic ceramic; (b) $V = 1170$ m/s, DOP = 26.2 mm for a 3×12.7 mm thick laminated ceramic structure; (c) $V = 1170$ m/s, DOP = 39.1 mm for a 6×6.35 mm thick laminated ceramic structure.

other two ceramic structures of the same total thickness. Thus, the laminated ceramic/polymer structure comprised of three 12.7 mm thick AlN tiles is observed to offer more resistance to penetration by a projectile than does a monolithic ceramic structure of the same total thickness. This has important implications in the design of lightweight ceramic armor.

4.3. Enhanced performance of the laminated ceramic/polymer structure

One of the main reasons for the enhanced penetration resistance of the laminated ceramic/polymer structure is the reduced wave propagation speed within the laminated ceramic structure when compared to an equivalent monolithic ceramic. Due to their low density and high stiffness, the speed of longitudinal sound waves in ceramics is generally of the order of 10 km/s. However, a periodic structure comprised of ceramic tiles bonded with thin polymer layers in between is dispersive in nature. In such structures, although the wave front moves at a phase velocity, c_p corresponding to the frequency of the repeated set in the chain, the peak stresses move at a significantly slower group velocity, c_g evaluated at that same frequency [24]. This difference between c_p and c_g is responsible for the spreading of the pulse leading to attenuation due to the periodicity of the structure. It should be noted that this attenuation of the shock wave due to the periodicity of the laminated ceramic/polymer structure is in addition to the attenuation due to radial spreading of the spherical wave front. The damage caused in the ceramic structure due to the passage of the compressive shock wave is expected to decrease with a decrease in the amplitude of the shock wave.

El-Raheb [24] performed a one-dimensional "elastic" analysis of transient wave propagation in a periodic stack of ceramic tiles bonded with thin polymer layers. By assuming that the ceramic tiles act as unconstrained rigid masses and that the polymer layers act as linear springs, El-Raheb [26] derived a relationship for the phase velocity c_p in the axial direction of a laminated stack as

$$c_p \cong c_b \left(\frac{\rho_b h_c}{\rho_c h_b} \right)^{1/2}, \tag{3}$$

where c_b is the speed of sound in the polymer, (ρ_b, h_b) is the polymer density and thickness, and (ρ_c, h_c) is the ceramic density and thickness. El-Raheb and Tham [27] performed an experimental investigation of the wave propagation in a periodic stack of AlN ceramic tiles bonded by thin weak silicone rubber layers and obtained a phase velocity of 3.7 km/s in the laminated ceramic structure. It should be noted that both c_p and c_g diminish with an increase in frequency, with a maximum at zero frequency (given by Eq. (3)). Thus, the sound waves travel at a significantly lower velocity in a laminated ceramic/polymer structure than in a monolithic ceramic material. This also leads to a lower velocity at which damage can propagate within the laminated ceramic structure, enhancing the target resistance (R_t) for the laminated ceramic/polymer structure. This is one of the main reasons for the better ballistic performance of the ceramic/polymer laminates comprised of three 12.7 mm thick ceramic tiles. Note that El-Raheb's analysis is elastic analysis and is not directly applicable to our case, which is governed by the fracture and failure in the ceramic material. However, we include it here to show that lamination can lead to a smaller damage velocity in a laminated ceramic structure. In a more recent experimental work on wave propagation in layered composites, Zhuang et al. [39] have investigated shock wave propagation in stainless steel, aluminum, and glass structures laminated with thin layers of polycarbonate in

between. Their results indicate that the shock wave velocity in a layered composite can be either between that of its components or lower than that of both components. Further, they show that the impedance mismatch of the interface contributes to the dissipation and dispersion of the shock waves. The larger the impedance mismatch between the components is, larger is the energy transported as internal energy, and hence the larger is the dissipation.

One of the other mechanisms that can possibly lead to the enhanced penetration resistance of a laminated ceramic/polymer structure is the crack arresting feature of the polymer layers in the laminated structure. As discussed in Section 2.2, it has been shown by other researchers (e.g., [40,41]) that brittle materials could be significantly toughened by introducing weak interfaces in the path of a growing crack to deflect the crack along the interface [42]. Note that this crack deflection phenomenon depends mainly on the ratio of the interface and cohesive fracture energies for the materials and the speed of propagating crack. Thus, it is possible that damage in the laminated ceramic/polymer structure is localized due to the attenuation of the stress waves (arising from the periodicity of the structure) and the deflection of the cracks at weak polymer interfaces. This would then lead to the enhanced penetration resistance of the laminated ceramic/polymer structures. Fig. 7 presents a post-test photograph of a polymer layer that was used to bond two adjacent ceramic tiles together. Extensive radial cracking in the polymer layer is observed which may be possibly due to crack deflection at the interface.

Note that the ballistic penetration experiments performed in this study are not suitable to identify the most dominant mechanism responsible for the enhanced penetration resistance of the

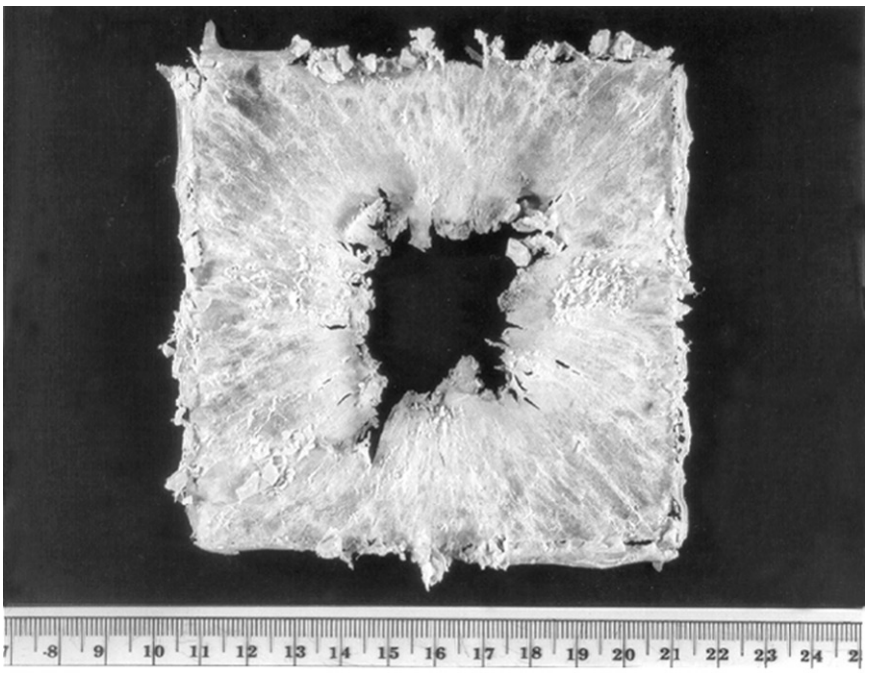

Fig. 7. Post-test photograph of a polymer layer that was used to bond two adjacent ceramic tiles together. Extensive radial cracking in the polymer layer is observed.

laminated ceramic/polymer structure. It is possible that all of the mechanisms mentioned earlier, viz. (a) attenuation of the stress waves due to the periodicity of the laminated structure, (b) reduced damage velocity in the laminated structure, and (c) the crack arresting feature of the polymer layer, are important factors that lead to the enhanced penetration resistance of the laminated ceramic/polymer structure. Further, well-designed experiments—which at this point have not been conceptualized, except that they cannot be the traditional ballistic experiments—are necessary to identify relative contribution of each of these mechanisms to ballistic performance of the laminated ceramic/polymer structures.

4.4. *Effect of ceramic tile thickness and polymer bond properties*

We now present a brief description of wave propagation and failure mechanisms in a laminated structure to increase our understanding of the influence of various material and geometrical parameters on the ballistic performance of laminated ceramic/polymer structures. This would also help us in understanding the reasons for the reduced penetration resistance of the laminated ceramic/polymer structures comprised of six 6.35 mm thick AlN tiles.

When a stress pulse is applied on top of a periodic stack, a compressive normal wave is generated under the footprint which disperses as it propagates across the thickness of the first ceramic tile. The difference in normal stress, σ_{zz} between the top and bottom faces of a ceramic layer, $\Delta\sigma_{zz}$, induces flexure in the form of anti-symmetric radial (σ_{rr}) and circumferential ($\sigma_{\theta\theta}$) stresses. At an interface, the wave is partly reflected and partly transmitted depending on the reflection and refraction coefficients [43]. A stiff polymer layer increases transmission and reduces $\Delta\sigma_{zz}$ which reduces flexure of the ceramic layer. On the other hand, a less stiff polymer layer decreases transmission and reduces coupling between the ceramic layers allowing more flexure of the top ceramic layers. Note that two competing damage mechanisms are operative in the component tiles of a laminated ceramic/polymer structure. The first mechanism is the damage in a ceramic tile due to the passage of the compressive shock wave. The second mechanism is the damage in a ceramic tile due to the bending stresses caused by the flexural waves. The optimum ceramic tile thickness and the polymer layer thickness and stiffness are the ones for which the probability of damage in a ceramic tile due to the two competing mechanisms is the same. One of the main reasons for the lower penetration resistance of the laminated structure comprised of six 6.35 mm thick ceramic tiles is the increased flexural damage in these thin tiles. Note that the damage mechanisms operative in brittle plates subjected to impact loading are strongly dependent on the thickness of the plate. For example, Ball [44] performed an experimental investigation of damage induced in laminated glass/polymer plates subjected to low-velocity impacts. He emphasized the importance of astute choice of plate thickness for optimal laminate design that would resist fracture by both contact stresses and bending stresses.

5. Summary

Ballistic penetration experiments have been performed on aluminum nitride (AlN) ceramic. Depth of penetration (DOP) experiments were conducted on monolithic and laminated ceramic/polymer structures of a constant total thickness of 38.1 mm. Experimental results demonstrate

that the penetration resistance of the laminated ceramic/polymer structure comprised of three 12.7 mm ceramic tiles is higher than that of the monolithic ceramic at comparable impact velocities. This is attributed to the attenuation of the stress waves due to the periodicity of the structure, reduced damage velocity, and the crack arresting feature of the polymer layer in the laminated ceramic/polymer structure. However, the relative contribution or significance of each of these mechanisms to ballistic performance could not be identified by the DOP tests. Further, well-designed experiments would be necessary to quantify the role of each of these mechanisms in enhancing the penetration resistance of the laminated ceramic/polymer structures. It is also observed that the penetration resistance decreases with further increase in layering (i.e., for six 6.35 mm ceramic tiles) due to damage caused by the increased flexure of the ceramic tiles.

Acknowledgements

This research was supported by the Dow Chemical Company which is gratefully acknowledged. The authors would like to express their sincere gratitude to Mr. S. Hanchak, Dr. M.J. Forrestal and Mr. E. Repacki for their assistance provided while setting up the experimental impact facility at Caltech.

References

[1] Matchen B. Applications of ceramics in armor products. Key Eng Mater 1996;122–124:333–42.
[2] Rosenberg Z, Yeshurun Y. The relation between ballistic efficiency and compressive strength of ceramic tiles. Int J Impact Eng 1988;7:357–62.
[3] Woodward RL. A simple one-dimensional approach to modeling ceramic composite armor defeat. Int J Impact Eng 1990;9(4):455–74.
[4] Sternberg J. Material properties determining the resistance of ceramics to high velocity penetration. J Appl Phys 1989;65:3417–24.
[5] Hornemann U, Rosenhausler H, Senf H, Kalthoff JF, Winkler S. Experimental investigation of wave and fracture propagation in glass slabs loaded by steel cylinders at high impact velocities. In: Harding J, editor. Mechanical properties at high rates of strain, 1984, pp. 291–98.
[6] Camancho, Ortiz M. Computational modelling of impact damage in brittle materials. Int J Solids Struct 1996; 33: 2899–2938.
[7] Curran DR, Seaman L, Cooper T, Shockey DA. Micromechanical model for comminution and granular flow of brittle material under high strain rate application to penetration of ceramic targets. Int J Impact Eng 1993;13: 53–83.
[8] Cortes R, Navarro C, Martinez MA, Rodriguez J, Sachez-Galvez V. Numerical modeling of normal impact on ceramic composite armors. Int J Impact Eng 1992;12(4):639–51.
[9] Ravichandran G, Subash G. A micromechanical model for high strain rate behavior of ceramics. Int J Solids Struct 1995;32:2627–46.
[10] Lankford J. Compressive strength and microplasticity in polycrystalline alumina. J Mater Sci 1977;12:791–6.
[11] Lankford J. Mechanisms responsible for strain-rate dependent compressive strength in ceramics. J Am Ceram Soc 1981;64.
[12] Longy F, Cagnoux J. Plasticity and microcracking in shock loaded alumina. J Am Ceram Soc 1989;72:971–9.
[13] Hauver G. Variation of target resistance during long rod penetration into ceramics. Proceedings of the 13th International Symposium on Ballistics, Stockholm, Sweden, 1992.

[14] Kanel GI, Rasorenov SV, Fortov VE. The failure waves and spallations in homogeneous brittle materials. In: Schmidt SC et al., editors. Shock Compression of Condensed Matter-1991. Amsterdam: Elsevier Science Publishing, 1992.
[15] Raiser GV, Cifton RJ. Failure waves in uniaxial compression of an aluminosillicate glass. In: Schmidt SC et al., editors. High Pressure science and Technology-1993. New York: AIP Press, 1994.
[16] Grady DE. Dynamic properties of ceramic materials, Technical Report No. SAND94-3266, Sandia National Laboratories, Albuquerque, New Mexico, 1995.
[17] Strassburger E, Senf H, Rosenhausler H. Fracture propagation during impact in three types of ceramics. J Phys IV 1994;C8:653–8.
[18] Subramanian R, Bless SJ. Penetration of semi-infinite AD995 alumina targets by tungsten long rod penetrators from 1.5 to 3.5 km/s. Int J Impact Eng 1995;17:807–16.
[19] Hegemeir GA, Nayfeh AH. A continuum theory for wave propagation in laminated composites. Case I: Propagation normal to the laminates. J Appl Mech 1973;40:503–10.
[20] Nayfeh AH, Nassar EA. Simulation of the influence of bonding materials on the dynamic behavior of laminated composites. J Appl Mech 1978;45:822–8.
[21] Sotiropoulos DA. Transmission of mechanical waves through laminated structures to evaluate interlamina bonds. Int J Mech Sci 1993;35:279–88.
[22] Brilllouin L. Wave propagation in periodic structures, 2nd ed.. New York: Dover, 1953.
[23] Robinson CW, Leppelmeir GW. Experimental verification of dispersion relations for layers composites. ASME J Appl Mech 1974;41:89–91.
[24] El-Raheb M. Transient elastic waves in finite layered media: one-dimensional analysis. J Accoust Soc Am 1993;95(6):3287–99.
[25] El-Raheb M, Wagner P. Transient elastic waves in finite layered media: two-dimensional axisymmetric analysis. J Acoust Soc Am 1996;99(6).
[26] El-Raheb M. Simplified analytic models for transient uniaxial waves in a layered periodic stack. Int J Solids Struct 1997;34(23):2969–90.
[27] El-Raheb M, Tham R. Transient waves in a periodic stack: experiments and comparison with analysis. J Acoust Soc Am.
[28] Cook J, Gordon JE. A mechanism for the control of crack propagation in all-brittle systems. Proc R Soc Lond A 1964;282:508.
[29] Kendall K. Transition between cohesive and interfacial failure in a laminate. Proc R Soc Lond A 1975;344:287.
[30] Lee W, Howard SJ, Clegg WJ. Growth of interface defects and its effect on crack deflection and toughening criteria. Acta Mat 1996;44(10):3905–22.
[31] Phillips AJ, Howard SJ, Clegg WJ, Clyne TW. The modeling and control of failure in bi-material ceramic laminates. J Phys IV 1993;3(C7):1875–81.
[32] Phillips AJ, Clegg WJ, Clyne TW. The failure of layered ceramics in bending and tension. Composites 1994;25:524–33.
[33] Chan HM. Layered ceramics: processing and mechanical behavior. Ann Rev Mater Sci 1997;27:249–82.
[34] Flocker FW, Dharni LR. Stresses in laminate glass subject to low-velocity impact. Eng Struct 1997;19(10):851–6.
[35] Flocker FW, Dharni LR. Modeling fracture in laminated architectural glass subject to low velocity impact. J Mat Sci 1997;32:2587–94.
[36] Franzen RR, Orphal DL, Anderson CE. The influence of experimental design on depth-of-penetration (DOP) test results and derived ballistic efficiencies. Int J Impact Eng 1997;19(8):727–37.
[37] Woodward RL, Gooch WA, O'Donnell RG, Perciballi WJ, Baxter BJ, et al. , A study of fragmentation in the ballistic impact of ceramics. Int J Impact Eng 1994;15(5):605–18.
[38] Anderson Jr CE, Walker JD, Bless SJ, Partom Y. On the l/d effect for long-rod penetrators. Int J Impact Eng 1996;18(3):247–64.
[39] Zhuang S, Ravichandran G, Grady DE. Experiments on shock wave propagation in periodically layered composites, J Mech Phy Solids, submitted for publication.
[40] Clegg WJ, Kendall K, Alford NM, Button TW, Birchall JD. A simple way to make tough ceramics. Nature 1990;347(6292):455–7.

[41] Clegg WJ. The fabrication and failure of laminar ceramic composites. Acta Metall Mater 1992;40:3085–93.
[42] Lee W, Clegg WJ. The deflection of cracks at interfaces. Materials 1996;116:193–208.
[43] Furlong JR, Westbury CF, Phillips EA. A method for predicting the reflection and refraction of spherical waves across a planar interface. J Appl Phys 1994;76(1):25–32.
[44] Ball A. The low velocity impact behavior of glass–polymer laminated plates. J Phys IV 1997;C3:921–6.